

# Nano-structure formation driven by local protonation of polymer thin films

Carsten Maedler\*<sup>a</sup>, Harald Graaf<sup>a</sup>, Sailaja Chada<sup>b</sup>, Mingdi Yan<sup>b</sup>, Andres La Rosa<sup>c</sup>  
<sup>a</sup>Institute of Physics, Chemnitz University of Technology, 09107 Chemnitz, Germany;  
<sup>b</sup>Department of Chemistry, Portland State University, Portland, OR 97201, USA;  
<sup>c</sup>Department of Physics, Portland State University, Portland, OR 97201, USA

## ABSTRACT

We report the creation of nano-structures via Dip Pen Nanolithography by locally exploiting the mechanical response of polymer thin films to an acidic environment. Protonation of cross linked poly(4-vinylpyridine) (P4VP) leads to a swelling of the polymer. We studied this process by using an AFM tip coated with a  $pH$  4 buffer. Protons migrate through a water meniscus between tip and sample into the polymer matrix and interact with the nitrogen of the pyridyl group forming a pyridinium cation. The increase in film thickness, which is due to Coulomb repulsion between the charged centers, was investigated using Atomic Force Microscopy. The smallest structures achieved had a width of about 40 nm. Different control experiments support our claim that the protonation is the reason for the swelling and therefore the formation of the structures. Kelvin probe force microscopy measurements suggest the presence of counter ions which compensate the positively charged pyridinium ions. We investigated the influence of the water meniscus on the structure formation by varying the relative humidity in the range from 5% to 60% for different dwell times. The diffusion of protons and counter ions is humidity-dependent and requires a water meniscus.

**Keywords:** P4VP, Dip Pen Nanolithography, Kelvin probe force microscopy

## 1. INTRODUCTION

Dip Pen Nanolithography (DPN) is a method for the direct deposition of molecules, also referred to as ink, from an AFM tip onto a substrate (Fig. 1).<sup>[1]</sup> It has been applied to create various nanoscale patterns of small molecules,<sup>[2]</sup> biological macromolecules,<sup>[3],[4]</sup> conducting polymers,<sup>[5]</sup> polymer single crystals,<sup>[6]</sup> inorganic materials<sup>[7],[8]</sup> and single atoms<sup>[9]</sup> on metals, semiconductors and monolayer functionalized surfaces. All these experiments are based on the adsorption of ink molecules on the sample surface.

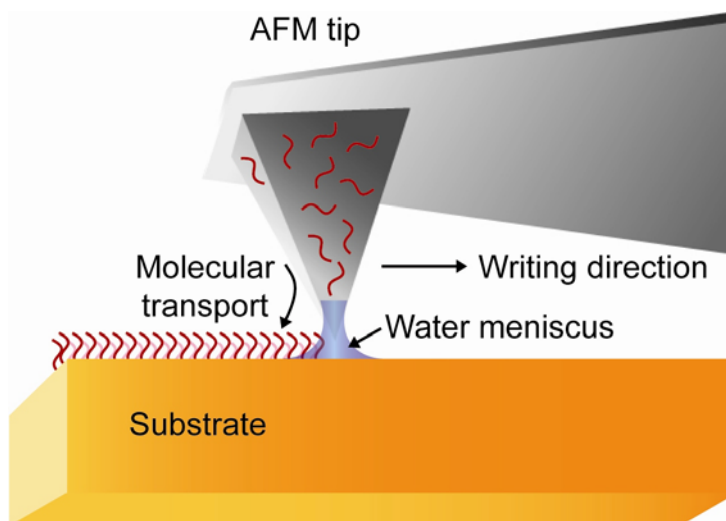


Fig. 1. Dip Pen Nanolithography principle. Molecules are transferred from an AFM tip onto the substrate. The diffusion rate of the molecules depends on the size of the water meniscus between tip and substrate.

There is still controversy about the influence of the water meniscus that builds up between an AFM tip and the substrate in DPN experiments. It was first visualized in real time by Schenk et al. using an environmental scanning electron microscope (ESEM).<sup>[10]</sup> Weeks et al. used the same method to study the dependence of the water meniscus size on the relative humidity (RH) for silicon and gold coated silicon substrates.<sup>[11]</sup> They observed no meniscus until 70% RH for the gold substrate and 80% RH for the silicon substrate within the resolution limit of the ESEM being about 50 nm. However, the height of the meniscus exhibits hysteresis, which means that when decreasing the RH they still observed a water meniscus at 40% RH for the silicon substrate, which did not change over a 10 min period. This hysteresis was also found by Petersen et al. who showed that the molecular transport rate (MTR) at a given humidity was less if data was collected when RH is increased than if collected at the same humidity as the RH is decreased.<sup>[12]</sup> They suggested a dry deposition of Mercaptohexadecanoic Acid (MHA), which is limited by surface diffusion and independent of RH up to a RH of about 50%. For humidities over 70% they noticed a sharp increase in MTR which they attributed to water meniscus bulk transport. In contrast to that, Rozhok et al. observed an increase in dot diameter already at a RH of as small as 10% when depositing MHA.<sup>[13]</sup> They proposed two competing humidity dependent factors that affect the rate of ink transport for MHA and octadecanethiol (ODT). One is the increasing meniscus size with increasing RH that allows for more molecules to be dissolved in the meniscus and therefore an increasing transport of molecules, the other one is an increasing blocking layer on the surface, which impedes ink transport. For the case of ODT they found the latter effect to be dominant leading to a decrease in dot diameter with increasing RH. In a different paper they suggested that even under dry conditions (RH < 1%) a water meniscus will form between an AFM tip and the substrate.<sup>[14]</sup> On the other hand, Schwartz claimed that the water meniscus is not responsible for the molecular transport of ODT and MHA to the substrate.<sup>[15]</sup> For ionic transport, however, he approved of a water-meniscus-driven molecular transport. Sheehan et al. demonstrated similar results for the deposition of ODT, where they showed that its diffusion coefficient is essentially unaffected by changes in RH.<sup>[16]</sup> In a new model proposed by Nafday et al. the ink transport of MHA occurs at the meniscus air-water interface.<sup>[17]</sup> This model was able to explain both the formation of ring structures of deposited MHA at high humidity and the independence of the dot size of ODT on the RH which is due to the hydrophobic nature of the self assembled monolayer of ODT which means that meniscus growth dynamics do not need to be considered.

In contrast to the DPN anchoring-molecule approach for creating nanostructures, we report on a DPN method that instead exploits the mechanical response of thin film poly (4-vinylpyridine) (P4VP) in an acidic environment. Several control experiments confirmed that an AFM tip, when coated with phosphate buffer solution of pH 4 and placed in contact with the substrate, delivers protons into the P4VP polymer film causing the latter to swell.<sup>[18]</sup> A similar result has been shown before in a macroscale setup, where an increase in film thickness of UV-cross-linked P4VP films under acidic stimulation was found.<sup>[19]</sup> This swelling is due to the protonation of pyridyl groups when adding Brønsted acids to form pyridinium ions, which was confirmed by infrared spectroscopy which showed a shift in the frequency band associated with the pyridyl ring-stretching modes to frequencies related to pyridinium ions. Mutual repulsions between the pyridinium ions cause the film to expand. Quartz crystal microbalance measurements suggested that water was absorbed in the swollen layer.

We show that the structure formation is water-meniscus-dependent by adjusting the RH to between 5% and 60%. Simultaneous imaging of the contact potential difference between tip and substrate using Kelvin probe force microscopy (KPFM)<sup>[20]</sup> enables us to monitor any charges embedded in the PV4P after protonation. An absence of the latter suggests that counter ions are absorbed during the protonation and compensate the positively charged pyridinium ions.

## 2. EXPERIMENTAL DETAILS

*Materials.* P4VP (molecular weight approximately 160 000, Aldrich), *n*-butanol (Fisher Scientific) were used as received. Sodium phosphate monobasic and sodium phosphate anhydrous dibasic were obtained from Mallinckrodt Chemical Works.

*Preparation of polymer thin films.* A 10 mg/ml solution of P4VP was prepared in *n*-butanol. Silicon wafers with a native oxide thickness of 10 Å were cut into 1 x 1 cm square pieces, cleaned by sonicating in isopropyl alcohol for 15 min, and subsequently dried under a stream of nitrogen. Afterward, a P4VP solution was spin coated onto the wafers at 2000 rpm for 60 s, followed by irradiation using a 450 W medium-pressure mercury lamp for 5 min (the latter included a 2 min warm-up time for the lamp to reach its maximal intensity). The 5.1 mW/cm<sup>2</sup> intensity of the lamp was measured using a sensor of peak sensitivity at a wavelength of 254 nm. The irradiated films were then soaked in *n*-butanol for 24 h to

remove the unbound polymer. The thickness of the film was measured with a Gaertner ellipsometer (model L116A, with a 2 mW He/Ne laser at an incident angle of  $70^\circ$ ), using as refractive indices 1.465 for  $\text{SiO}_2$  and 1.581 for P4VP in the final estimations. The average of measurements at three different locations gave a typical thickness of  $37 \pm 2$  nm.

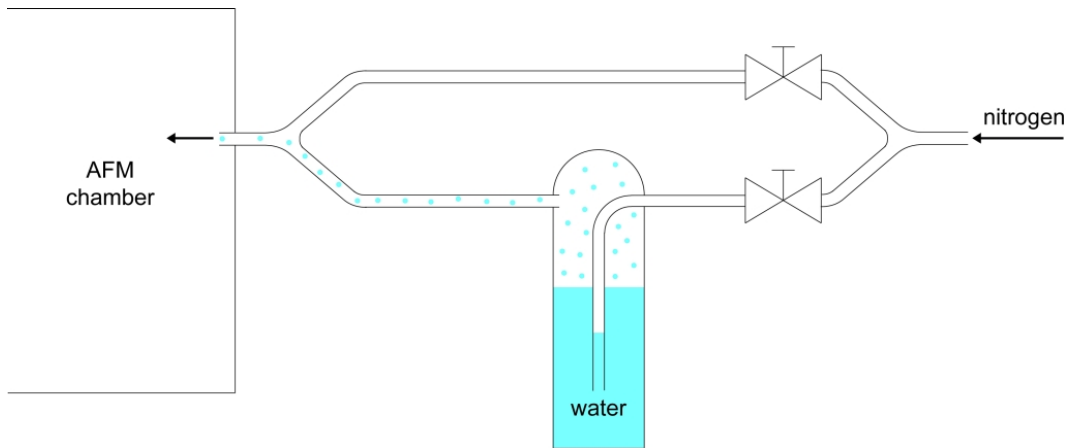


Fig. 2. System for the RH control in the environmental chamber enclosing the AFM. A stream of dry nitrogen was either fed into the chamber directly or bubbled through ultra pure water in a parallel channel before being merged with the nitrogen stream entering the chamber.

*Preparation of the AFM tip.* Phosphate buffer solution (0.1M) of pH 4 was prepared using  $\text{NaH}_2\text{PO}_4$  and  $\text{Na}_2\text{HPO}_4$ . AFM tips (Si, NSC 15, Mikromasch,  $k=40$  N/m) were coated by simply immersing the probe into the buffer solution for 1 min, and then allowing them to dry in air for 10 min. Subsequently, the tip was mounted on the head stage of a multimode scanning probe microscope (Nanoscope III, Veeco). For the KPFM and the RH-dependent measurements an Anfattec Level AFM was used, which was enclosed by an environmental chamber. A two-way system, which is shown in Fig. 2, was used for the humidity control. A stream of dry nitrogen was either fed into the chamber directly or bubbled through ultra pure water in a parallel channel before being merged with the nitrogen stream entering the chamber. The RH was measured using a humidity sensor from Sensirion (SHT75, accuracy  $\pm 2\%$  RH). In a given session, the same tip was used for all the intended test experiments but cleaned and coated anew before each trial. In order to verify that the starting substrate topography was smooth enough, all the samples were first scanned (with the buffer coated tip) at a relatively fast scan rate (2 Hz or  $5 \mu\text{m/s}$ ) and in tapping mode (TM). The use of high scanning rates prevented transferring buffer molecules to the surface. Subsequently, line and dot structures were fabricated using slower scanning rates (as detailed below). A step by step process of the polymer pattern formation is outlined in Fig. 3.

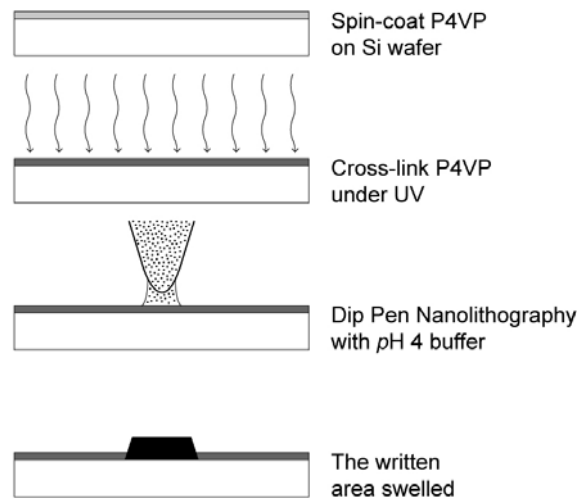


Fig. 3. Procedure for implementing spatially localized protonation and swelling of a P4VP polymer film via DPN.

### 3. RESULTS AND DISCUSSION

#### 3.1 Force Dependence

Line structures were created by scanning the sample in contact mode (CM) with the tip being retracted after each line and being placed on a different spot of the substrate to write another line. Applying different contact forces to the tip resulted in different heights of the structures as can be seen in Fig. 4. The applied forces are 1, 2 and 3  $\mu\text{N}$ , which led to structure heights of 7, 12 and 25 nm, respectively. These forces are rather high compared to other DPN experiments and lead to scratches on the same substrate when the tip was not coated with the pH 4 buffer solution prior to scanning in CM (not shown here). A penetration of the tip into the polymer thin film is therefore needed to increase its height by protonation. With an increasing contact force the tip penetrates deeper into the polymer which leads to a larger area of interaction between the tip and the polymer and a resulting increase in number of transferred molecules.

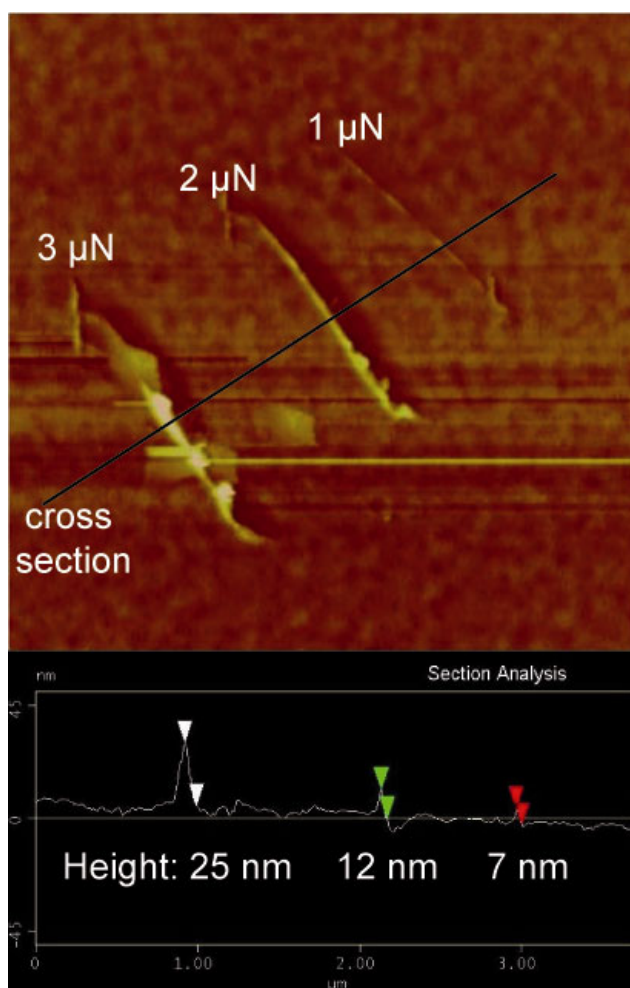


Fig. 4. Lines of different heights on P4VP thin films could be created using an AFM tip coated with a pH 4 buffer solution when applying different contact forces to the tip. The applied force is indicated at the created structures.

### 3.2 Charge Detection

Imaging previously protonated P4VP in KPFM did not show any changes in contact potential difference (CPD) between the swollen and the untreated part of the polymer. Given that already very few charges can be detected using KPFM<sup>[21]</sup> this result indicates that counter ions are embedded in the polymer which compensate the positive charge of the pyridinium ions. The counter ions in our case are  $\text{HPO}_4^{2-}$  molecules from the phosphate buffer solution. An additional partial screening of the charge by water molecules is likely since quartz crystal microbalance measurements described in a previous paper suggested that water was absorbed in the swollen layer. The proposed swelling mechanism and incorporation of water molecules and  $\text{HPO}_4^{2-}$  counter ions is depicted in Fig. 5.

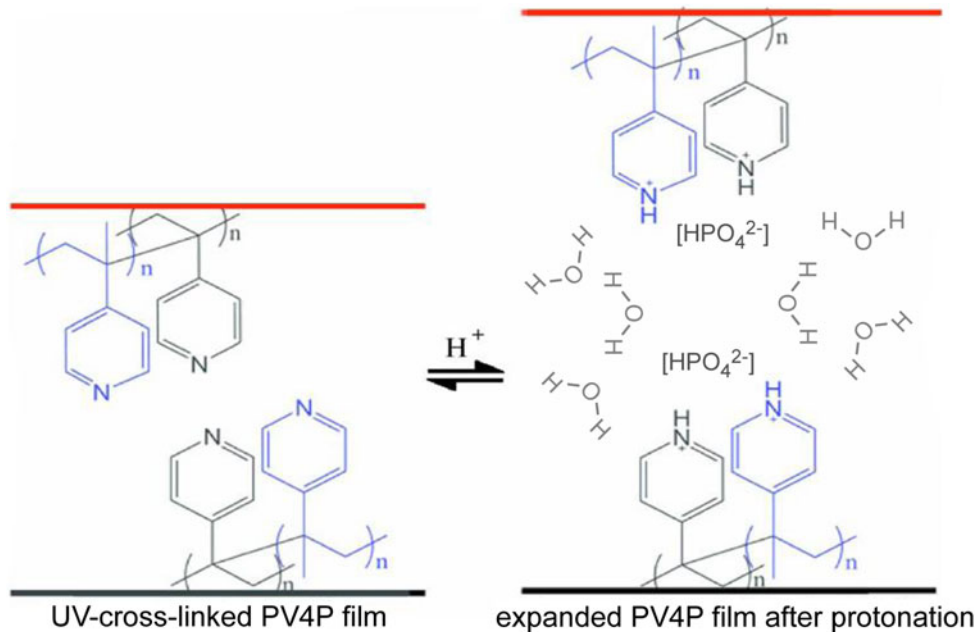


Fig. 5. Proposed swelling mechanism. Coulomb repulsion between the pyridinium ions leads to an increase of the film thickness. The voids are filled with water molecules and counter ions.

### 3.3 Dwell Time Dependence

To get information about the transport mechanism of the molecules we brought the coated tip in contact with the polymer surface and left it there for a certain amount of time before retracting it and repeating the procedure at a different spot. The height of the dot-like structures created in this way increased with increasing dwell time (Fig. 6). This indicates a diffusion-type phenomenon. More molecules get transferred from the tip to the sample when the tip is in contact with the substrate for a longer period of time. For longer dwell times the height of the structures goes into a saturation, which can be understood in terms of the finite thickness of the film and therefore a maximum capability to swell.

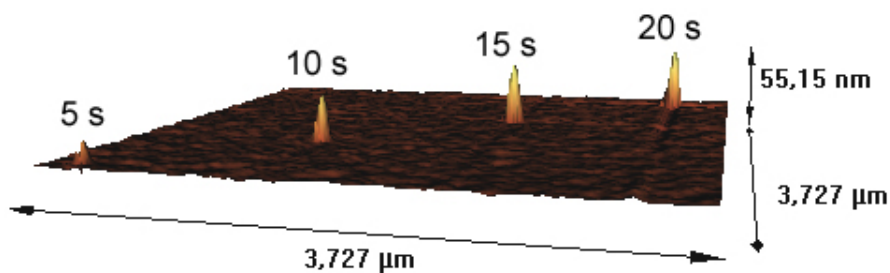


Fig. 6. Dots were created by leaving the coated tip in contact with the substrate for different amounts of time. The dwell time is indicated above the peaks.

### 3.4 Humidity Dependence

Again dot-like structures were created while varying the relative humidity inside of the AFM chamber. Attention was paid to a possible hysteresis effect<sup>[10]</sup> by starting at 60% RH and subsequent continuous decrease of the RH. Dots were written at 60%, 50% and 40% RH, respectively. No structures could be created for RH below 30%. This means that the transfer of the buffer molecules from the tip to the surface requires a sufficient water meniscus between tip and sample. Buffer molecules probably dissolve in the water before diffusing into the polymer. Without dissolution no molecules can be transferred to the substrate. With decreasing RH the height of the structures decreases, which indicates that the water meniscus becomes smaller. This was already seen by Schenk et al.<sup>[10]</sup> A smaller water meniscus leads to fewer dissolved buffer molecules and therefore a lower rate of protonation of the pyridyl groups. The results are summarized in the graph in Fig. 7.

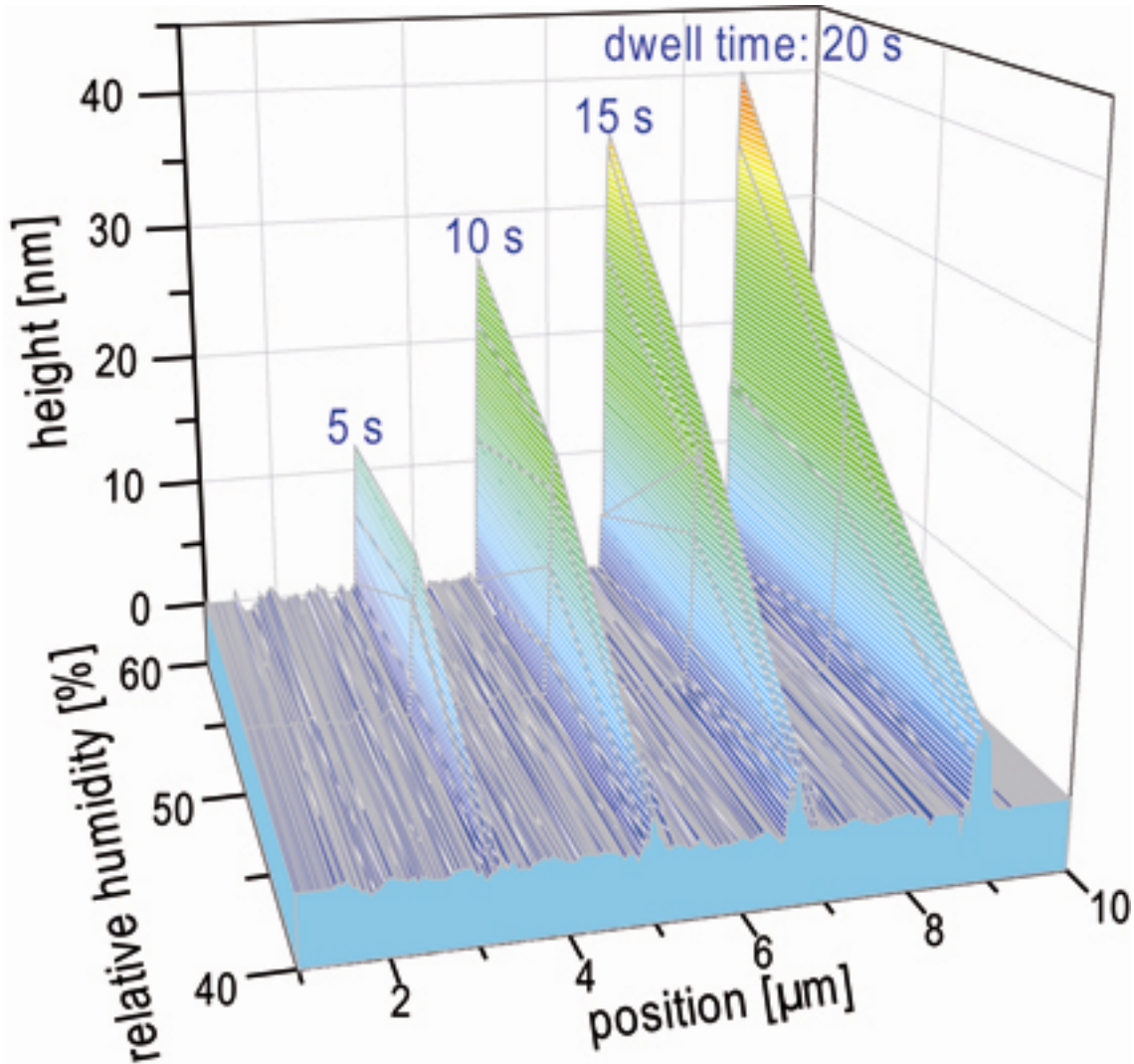


Fig. 7. Structure height against dwell time and relative humidity. The dwell time is indicated above the peaks.

## 4. CONCLUSION

We have demonstrated the creation of nanostructures by protonation of P4VP thin films and a resulting swelling of the polymer by delivering molecules from an AFM tip coated with a pH 4 buffer solution. The transfer of the molecules strongly depends on the RH and therefore the water meniscus between tip and sample. The writing mechanism is not fully understood but it seems to be crucial that the tip penetrates the surface for successful protonation. A diffusion-type phenomenon was observed for the structure formation. No change in contact potential difference for the swollen polymer suggests that water molecules and counter ions are embedded in the protonated polymer and screen the positive charge of the pyridinium ions.

## ACKNOWLEDGEMENT

M. Y. acknowledges the financial support from the donors of the Petroleum Research Fund, administered by the American Chemical Society (PRF #43469 AC7), and NIH through an AREA Award GM066279. A. L. R. acknowledges support from the USA Air Force Office of Scientific Research through Grant No. FA9550-07-1-0511, and by the Oregon Nanoscience and Microtechnologies Institute through Grant No. N00014-07-1-0457. H. G. acknowledges financial support by the deutsche Forschungsgemeinschaft (GR 2659/4-1).

## REFERENCES

- [1] Piner, R. D., Zhu, J., Xu, F., Hong, S. and Mirkin, C.A. "'Dip-Pen' Nanolithography," *Science* 283, 661-663 (1999).
- [2] Hong, S., Zhu, J. and Mirkin, C. A., "Multiple Ink Nanolithography: Toward a Multiple-Pen Nano-Plotter," *Science* 286, 523-525, (1999).
- [3] Noy, A., Miller, A. E., Klare, J. E., Weeks, B. L., Woods, B. W. and DeYoreo, J. J., "Fabrication of Luminescent Nanostructures and Polymer Nanowires Using Dip-Pen Nanolithography," *Nano Lett.* 2(2), 109-112 (2002).
- [4] Demers, L. M., Ginger, D. S., Li, Z., Park, S.-J., Chung, S.-W. and Mirkin, C. A., "Direct Patterning of Modified Oligonucleotides on Metals and Insulators by Dip-Pen Nanolithography," *Science* 296, 1836-1838 (2002).
- [5] Maynor, B. W., Filocamo, S. F., Grinstaff, M. W. and Liu, J., "Direct-Writing of Polymer Nanostructures: Poly(thiophene) Nanowires on Semiconducting and Insulating Surfaces," *J. Am. Chem. Soc.* 124(4), 522-523 (2002).
- [6] Liu, X., Zhang, Y., Goswami, D. K., Okasinski, J. S., Salaita, K., Sun, P., Bedzyk, M. J. and Mirkin, C. A., "The Controlled Evolution of a Polymer Single Crystal," *Science* 307, 1763-1766 (2005).
- [7] Liu, X., Fu, L., Hong, S., Dravid, V. P. and Mirkin, C. A., "Arrays of Magnetic Nanoparticles Patterned via "Dip-Pen" Nanolithography," *Adv. Mater.* 14(3), 231-234 (2002).
- [8] Su, M., Liu, X., Li, S.-Y., Dravid, V. P. and Mirkin, C. A., "Moving beyond Molecules: Patterning Solid-State Features via Dip-Pen Nanolithography with Sol-Based Inks," *J. Am. Chem. Soc.* 124(8), 1560-1561 (2002).
- [9] Wang, Y., Zhang, Y., Li, B., Lü, J. and Hu, J., "Capturing and depositing one nanoobject at a time: Single particle dip-pen nanolithography," *Appl. Phys. Lett.* 90(13), 133102(2pp) (2007).
- [10] Schenk, M., Fütting, M. and Reichelt, R., "Direct visualization of the dynamic behavior of a water meniscus by scanning electron microscopy," *J. Appl. Phys.* 84(9), 4880-4884 (1998).
- [11] Weeks, B. L., Vaughn, M. W. and DeYoreo, J. J., "Direct Imaging of Meniscus Formation in Atomic Force Microscopy Using Environmental Scanning Electron Microscopy," *Langmuir* 21(18), 8096-8098 (2005).
- [12] Peterson, E. J., Weeks, B. L., DeYoreo, J. J. and Schwartz, P. V., "Effect of Environmental Conditions on Dip Pen Nanolithography of Mercaptohexadecanoic Acid," *J. Phys. Chem. B* 108(39), 15206-15210 (2004).
- [13] Rozhok, S., Piner, R. and Mirkin, C. A., "Dip-Pen Nanolithography: What controls Ink Transport?," *J. Phys. Chem. B* 107(3), 751-757 (2003).
- [14] Rozhok, S., Sun, P., Piner, R., Lieberman, M. and Mirkin, C. A., "AFM Study of Water Meniscus Formation between an AFM Tip and NaCl Substrate," *J. Phys. Chem. B* 108(23), 7814-7819 (2004).
- [15] Schwartz, P. V., "Molecular Transport from an Atomic Force Microscope Tip: A Comparative Study of Dip-Pen Nanolithography," *Langmuir* 18(10), 4041-4046 (2002).
- [16] Sheehan, P. E. and Whitman, L. J., "Thiol Diffusion and the Role of Humidity in "Dip Pen Nanolithography"," *Phys. Rev. Lett.* 88(15), 156104(4pp) (2002).
- [17] Nafday, O. A., Vaughn, M. W. and Weeks, B. L., "Evidence of meniscus interface transport in dip-pen nanolithography: an annular diffusion model," *J. Chem. Phys.* 125(14), 144703(4pp) (2006).

- [18] Maedler, C., Chada, S., Cui, X., Taylor, M., Yan, M. and La Rosa, A., "Creation of nanopatterns by local protonation of P4VP via dip pen nanolithography," *J. Appl. Phys.* 104(1), 014311 (4pp) (2008).
- [19] Harnish, B., Robinson, J. T., Pei, Z., Ramstrom, O. and Yan, M., "UV-Cross-Linked Poly(vinylpyridine) Thin Films as Reversibly Responsive Surfaces," *Chem. Mater.* 17(16), 4092-4096 (2005).
- [20] Nonnenmacher, M., O'Boyle, M.P. and Wickramasinghe, H.K., "Kelvin Probe Force Microscopy," *Appl. Phys. Lett.* 58(25), 2921-2923 (1991).
- [21] Terris, B. D., Stern, J. E., Rugar, D. and Mamin, H. J., "Contact Electrification Using Force Microscopy," *Phys. Rev. Lett.* 63(24), 2669-2672 (1989).